Kinetic and Thermodynamic Analysis of Liquid-Phase Benzene Hydrogenation

Utpal K. Singh and M. Albert Vannice
Chemical Engineering Dept., Pennsylvania State University, University Park, PA 16802

Liquid-phase benzene hydrogenation on Pd/η-Al_2O_3 *catalysts was studied between 358 and 488 K and over an* H_2 *pressure range of 7 to 54 atm. Kinetic data were obtained under differential reaction conditions that were free of all transport limitations, thus allowing the development of a kinetic model that could be compared to that for the vapor-phase reaction. In contrast to vapor-phase studies at 1 atm, no activity maximum was observed during liquid-phase hydrogenation between 358 and 493 K and at 54-atm* H_2 *pressure. A model that invokes dissociative, noncompetitive* H_2 *adsorption, addition of the first H atom as the rate-determining step, and a concurrent dehydrogenated benzene surface species was consistent with experimental observations. The fitted parameters were thermodynamically consistent and agreed with those from previous vapor-phase studies. In addition, thermodynamic analysis of the quasi-equilibrated hydrogen adsorption process indicates that in the presence of solvent effects, increasing hydrogen solubility in the liquid phase can increase the surface coverage of hydrogen. In the absence of any solvent effect, however, surface coverage depends only on the partial pressure of hydrogen and is independent of the nature of the solvent. Furthermore, when solvent effects exist, use of the liquid-phase hydrogen concentration in the rate expression yields a solvent-independent adsorption equilibrium constant, while in the absence of solvent effects,* P_{H_2} *should be used in the rate expression to acquire this parameter.*

Introduction

Considerable effort has been made to better understand the kinetics of vapor-phase benzene hydrogenation on supported Group VIII metals (Mirodatos et al., 1987; van Meerten et al., 1976, 1977, 1979; van Meerten and Coenen, 1975; Chou and Vannice, 1987; Lin and Vannice, 1993). Benzene hydrogenation is of industrial relevance because its reaction product, cyclohexane, is an important industrial intermediate used in the production of Nylon-6 and Nylon-66 (Hancock, 1975). In addition, increasing environmental awareness has resulted in the need to remove benzene, a known carcinogen, from solvents and transportation fuels (Toppinen, 1996). Kinetic modeling and surface-science studies have provided much insight about the reaction in the vapor phase; however, much less is known about the liquid-phase reaction, although it has been studied to some extent, with emphasis placed on the selectivity issues relating to formation of cyclohexene (Struijk and Scholten, 1992; Struijk et al., 1992a; Odenbrand and Lundin, 1980; Nagahara et al., 1997), an intermediate in benzene hydrogenation. Toppinen et al. (1996, 1997), Temkin et al. (1989), and Konyukhov et al. (1987) have studied liquid-phase benzene hydrogenation over supported Ni, Pd, and Pt catalysts with a focus on obtaining quantitative kinetic data. However, no turnover frequencies (TOFs), that is, reaction rates normalized to number of surface metal atoms, were reported in these investigations. In addition, comparison of liquid-phase vs. vapor-phase kinetics was difficult, since the former reactions were not conducted in a differential mode, and the enthalpies and entropies of adsorption for H_2 and benzene have not been reported, making the evaluation of the thermodynamic consistency of the fitted parameters difficult.

Solvent effects have frequently been reported for liquid-phase hydrogenation reactions and related to properties, such as the dielectric constant and cohesive energy density, among

---

Correspondence concerning this article should be addressed to M. A. Vannice.

others (Augustine, 1976; Eckert et al., 1974; Wong and Eckert, 1969). In addition, solvent effects have also been introduced by the competitive adsorption of the solvent with reactants that can influence the reaction rates and selectivities (Struijk et al., 1992; Augustine and Techasauvapak, 1994). Few studies exist that examine the influence of hydrogen solubility on the reaction kinetics. Rajadhyaksha and Karwa (1986) studied liquid-phase hydrogenation of *o*-nitrotoluene and attributed the change in reaction rates in different solvents to thermodynamic interactions that were quantified using activity coefficients. Madon et al. (1978) studied liquid-phase hydrogenation of cyclohexene over supported Pt catalysts and found that liquid-phase hydrogen concentration, rather than H_2 partial pressure, was the better choice for use in the reaction-rate expression. This was reinforced by Boudart and Sajkowski's (1991) study of liquid-phase cyclohexene hydrogenation over supported Rh catalysts.

In the present work, we studied the liquid-phase hydrogenation of benzene on three $Pd/\eta\text{-}Al_2O_3$ catalysts under differential reaction conditions (up to 20% conversion) for the purpose of kinetic modeling and comparison to vapor-phase studies. Various experimental tests were conducted to verify that no transport limitations existed under the reaction conditions utilized. Finally, it is shown by thermodynamic equilibrium arguments, in agreement with Madon et al. (1978), that due to interactions of the solvent with the reacting system, the use of H_2 concentration in the liquid phase is preferred over H_2 pressure in the rate expression because solvent-independent adsorption equilibrium constants are obtained as parameters. In addition, it is also shown that with quasi-equilibrated adsorption of hydrogen, nonideal effects imposed by the solvent can increase the surface coverage of hydrogen as the hydrogen solubility increases at a constant partial pressure of hydrogen in the gas phase.

Experimental Studies

Catalyst synthesis and characterization

The $\eta\text{-}Al_2O_3$ support was prepared by calcination of β-alumina trihydrate (Exxon Research and Engineering Co., 245 m^2/g) at 873 K for 4 h. Catalysts were prepared by an incipient wetness technique using H_2PdCl_4 (Ventron) dissolved in dilute hydrochloric acid solution and added drop-wise (0.5 cc/g Al_2O_3) with stirring to the dried support. The impregnated catalysts were dried for 12 h at 393 K and stored in a desiccator for later use. Metal loadings were obtained by DC plasma emission spectroscopy.

Hydrogen chemisorption was performed in a stainless-steel UHV system with an ultimate vacuum of 10^{-7} torr. Details of the procedure are described elsewhere (Palmer and Vannice, 1980). Briefly, *in-situ* reduction at 723 K for one hour was followed by evacuation at 673 K and finally cooling to room temperature under vacuum. Measurements were performed at 300 K in the pressure range of 100–300 torr using 99.999% H_2 (MG Industries) that was further purified by passing through an Oxytrap (Alltech). Two consecutive isotherms, separated by a 30-min evacuation period, were obtained. Pd dispersions were calculated using irreversible uptakes and assuming a stoichiometry of $H_{irr}/Pd_{surf} = 1$. Table 1 displays the results of H_2 chemisorption on the $Pd/\eta\text{-}Al_2O_3$ catalysts.

Table 1. H_2 Chemisorption Results at 300 K

Catalyst	H_2 Chemisorption (μmol H/g Cat.)			Dispersion	
	H_{total}	H_{rev}	H_{irr}	H/Pd	H_{rev}/Pd
0.08% $Pd/\eta\text{-}Al_2O_3$	5	2	3	0.40	0.4
0.94% $Pd/\eta\text{-}Al_2O_4$	83	39	44	0.50	0.9
1.20% $Pd/\eta\text{-}Al_2O_5$	69	40	29	0.25	0.74

Hydrogenation reactions

Benzene hydrogenation reactions were conducted in a 100-mL stainless-steel autoclave (EZ-Seal Autoclave Engineers) operated in a semibatch mode. Hydrogen (MG Industries, 99.999%) was further purified by a high-pressure Oxytrap (Alltech), while He (MG Industries, 99.999%) was used as received. Figure 1 shows the reaction system utilized in the present study. This configuration allows *in-situ* reduction of the catalyst up to 773 K and addition of liquid reactants and solvents into the reactor via a syringe pump (ISCO 500D) without exposure to air. A gas-handling system was developed to control pressure and monitor flow rates during reaction and catalyst pretreatment. A mass-flow controller (Brooks 5850E) was used for controlling the He flow rate (0–200 SCCM) during catalyst pretreatment; while a mass-flow sensor (Brooks 5860E) and a proportional/integral pressure controller (Brooks 5866) were used in series to monitor the rate of H_2 uptake and maintain constant H_2 pressure to within $\pm 1\%$ of the setpoint. The mass-flow sensor monitored the flow of H_2 into the reactor and stored the data in a computer for analysis. The pressure controller and mass-flow sensor (PC-MFS) system were controlled by a digital control/readout unit (Brooks 0154E), from which data could be extracted at a maximum rate of 15 data points per second.

Additionally, a series of experiments was performed at 54-atm hydrogen pressure with 60 mol % benzene in hexane with 1.2% $Pd/\eta\text{-}Al_2O_3$ over a temperature range of 358 K to 493 K to check for a temperature maximum. Fresh catalyst samples were utilized for reactions performed at 358 K, 388 K, 408 K, and 493 K. TOFs at 443 K and 473 K were obtained on the same catalyst sample.

Results

Table 1 shows the H_2 chemisorption results for different Pd catalysts. The metal dispersions varied from 0.25 to 0.50 for these catalysts, while the concentration of surface metal atoms varied by more than an order of magnitude (from 3.0 μmoles Pd_s/g cat. to 44 μmoles Pt_s/g cat.). The Madon-Boudart (1982) test was conducted to evaluate the significance of heat and mass-transfer effects. In the absence of such limitations, the rate of a structure-insensitive reaction is proportional to the concentration of active sites, thus yielding a constant TOF (initial rate of benzene disappearance normalized to number of surface Pd atoms) for catalysts with varying numbers of exposed surface metal atoms. Results of this test are displayed in Table 2 for a reaction with 60 mol % benzene in hexane at 13.6 atm H_2 pressure and temperatures of 388 K, 408 K, and 448 K. The similarity among TOFs at three different temperatures verifies the absence of not only internal and external mass transfer, but also heat-trans-

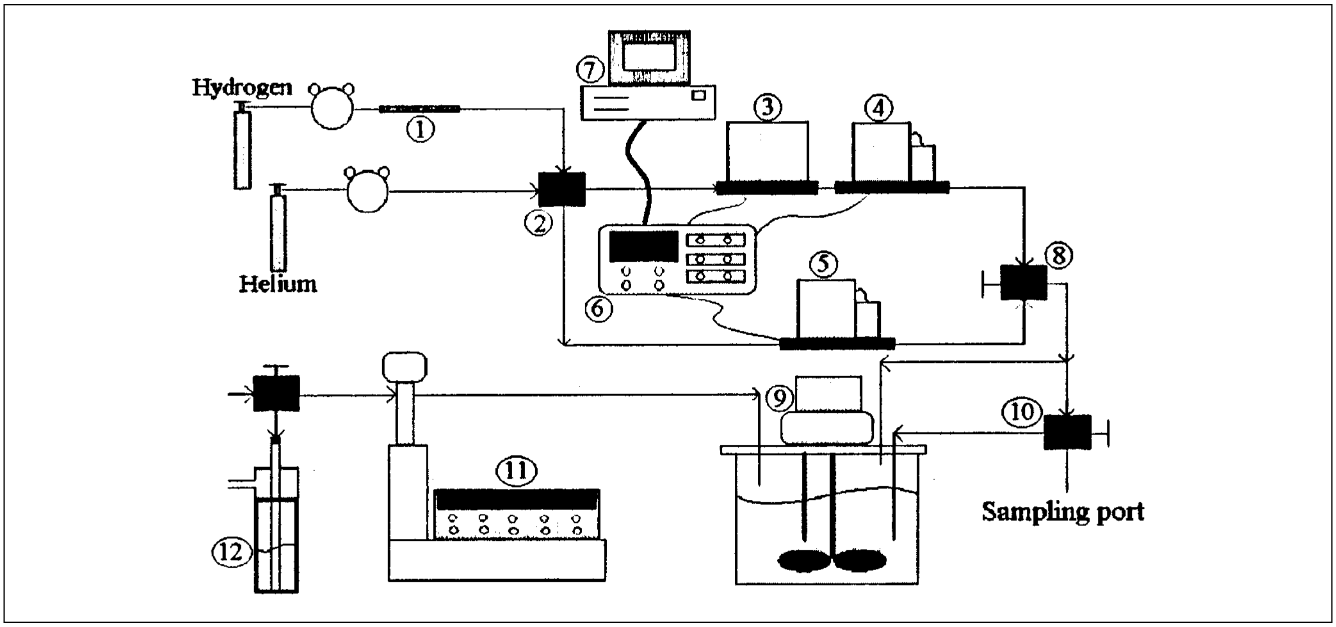

Figure 1. Reactor system utilized in the present study.

1: Oxytrap; 2: 4-way valve; 3: mass-flow controller; 4: pressure controller; 5: mass-flow controller; 6: modular control and readout unit; 7: computer to record pressure and mass flow; 8: 3-way valve; 9: stainless-steel autoclave; 10: 3-way sampling valve; 11: high-pressure syringe pump; 12: sample addition vessel.

fer limitations (Madon and Boudart, 1982). The activation energies for the 0.08%, 0.94%, and 1.2% Pd/η-Al_2O_3 catalysts were 5.5 kcal/mol, 6.8 kcal/mol, and 6.9 kcal/mol, respectively. The absence of external diffusion limitations was further verified by changing the stirring speed from 500 rpm to 1,700 rpm and monitoring the reaction at 408 K and 27.2 atm via the H_2 uptakes, as shown in Figure 3. The constancy of TOFs exhibited by catalysts with different concentrations of exposed metal surface atoms and the invariance of the rate with stirring speeds greater than 500 rpm are verification of the absence of transport processes under the reaction conditions in the present study.

Further support for the validity of the reaction rates reported in this study is obtained by comparison with data reported by Konyukhov et al. (1987) for liquid-phase benzene hydrogenation, free of transport limitations, over Pd supported on activated carbon. While TOFs were not explicitly reported in their study, an estimate can be obtained by utilizing their H_2 chemisorption results. A TOF of 0.49 s^{-1} at 403 K and 29.6 atm was calculated from the data reported by these authors (Konyukhov et al., 1987) compared to 0.54 s^{-1} in the present study. At 383 K and 10 atm, a TOF of 0.04 s^{-1} was calculated (Konyukhov et al., 1987) compared to 0.08 s^{-1} in the present study.

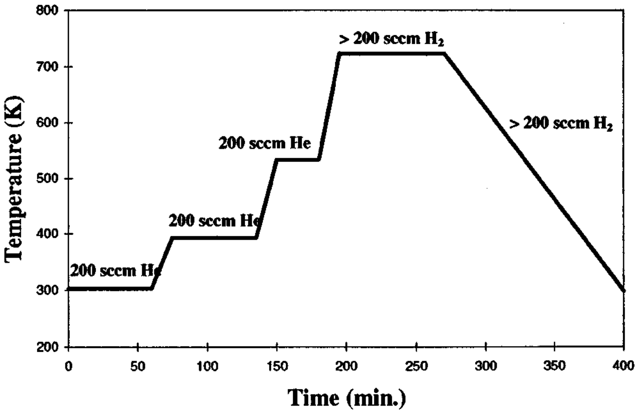

Figure 2. Temperature profile for *in-situ* pretreatment of catalysts.

The use of a stainless-steel reactor raises the question of leaching of metals from the reactor walls into the solution and possible poisoning of the catalyst. Elemental analysis of the used liquid-phase reaction mixture as well as a used catalyst sample revealed no detectable concentration of metals in either phase. This information is consistent with negligible deactivation observed and the reproducibility of data from run to run.

Figure 4 compares reaction rates based on GC data to those obtained from the continuous H_2 uptakes. The pressure controller and mass-flow sensor (PC-MFS) data reveal a decrease in rate during the course of the reaction. The tempo-

Table 2. Madon–Boudart Test for the Absence of Heat and Mass-Transfer Effects at 200 psia Hydrogen Pressure and 60 mol % Benzene in Hexane

Temp. (K)	TOF (s^{-1}) 0.08% Pd/η-Al_2O_3	TOF (s^{-1}) 0.94% Pd/η-Al_2O_3	TOF (s^{-1}) 1.20% Pd/η-Al_2O_3
388	0.11	0.07	0.13
408	0.23	0.22	0.20
448	0.30	0.26	—

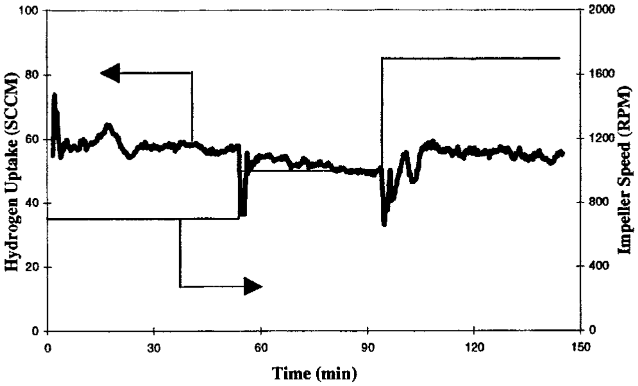

Figure 3. Stirring-speed study to evaluate the absence of external mass-transfer resistance during benzene hydrogenation using 1.2% Pd/η-Al_2O_3 catalyst at 408 K, 27 atm H_2, and neat benzene.

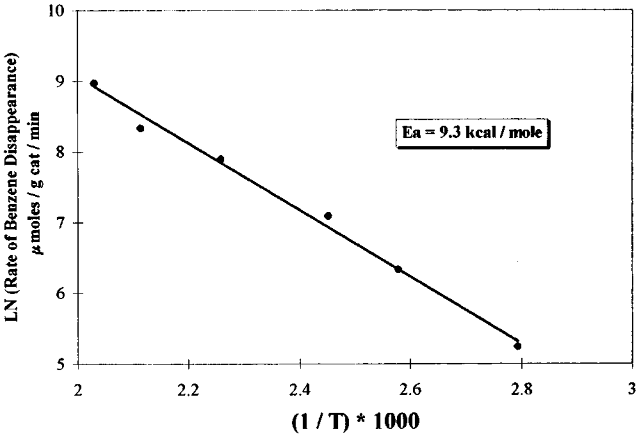

Figure 5. Arrhenius plot for benzene hydrogenation over 1.29 Pd/η-Al_2O_3 at 54 atm H_2 using 60 mol % benzene in hexane.

ral conversion profile, however, indicates constant rate during the entire course of the reaction. If the rate of H_2 uptake is evaluated using benzene conversion data (from GC results) during the first 200 min, a value of 0.93 mmol/min is obtained compared to an average value of approximately 1.0 mmol/min from the PC-MFS system. Similarly, if the hydrogen uptake is evaluated from the benzene conversion data (from GC results) during the last 100 min, a reaction rate of 0.75 mmol/min is obtained compared to an average rate of about 0.60 mmol/min from the PC-MFS data. Thus, the continuous, automated rate-acquisition system yields accurate and reliable data during the course of the reaction that can distinguish subtle changes in the reaction rate that would otherwise have been difficult to detect using the concentration data alone. In addition, it is interesting to note that no significant catalyst deactivation was detected over the 6-h reaction time during which complete conversion of benzene was achieved. The noticeable decrease in rate near the end can be attributed to the marked reduction in benzene concentration.

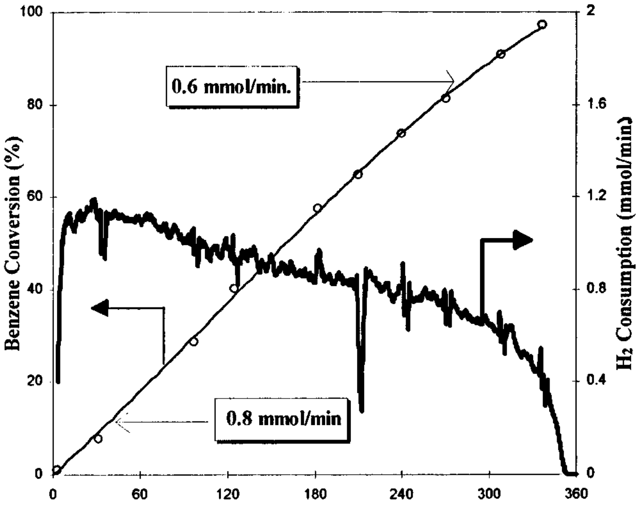

Figure 4. Reaction rates from temporal concentration data (open circles) and H_2 uptake results (heavy solid lines) for reaction over 0.94% Pd/η-Al_2O_3 at 408 K, 27 atm using 35 mol % benzene in hexane.

Figure 5 shows a typical Arrhenius plot for hydrogenation of 60 mol % benzene in hexane at 54 atm over 1.2% Pd/η-Al_2O_3, which yields an activation energy of 9.3 kcal/mol. In contrast with vapor-phase studies at 1 atm H_2 pressure, where an activity maximum has frequently been reported near 453 K (van Meerten et al., 1976; Chou and Vannice, 1987b; Lin and Vannice, 1993a), no such behavior was observed in the present study. Activity maxima, however, have been reported for liquid-phase hydrogenation of benzene on unsupported Ru catalysts ($RuCl_3$) at 463 K and 34 atm H_2 pressure in the presence of NaOH (15).

Figure 6 shows the effect of benzene concentration and liquid-phase H_2 concentration on the rate of benzene hydrogenation in hexane using a 1.2% Pd/η-Al_2O_3 catalyst. The reaction rate was near zero order in benzene concentration and between one-half to first-order in liquid-phase hydrogen concentration. The solid lines represent the fit of the kinetic model (described later) to the experimental data.

Discussion

Previous vapor-phase studies of benzene hydrogenation over supported Pd catalysts yielded a kinetic model invoking dissociative adsorption of H_2, noncompetitive adsorption between H_2 and benzene, and a concurrent dehydrogenation reaction to form a hydrogen-deficient phenyl surface species. No rate-determining step was assumed, which resulted in a complex model, but one that exhibited thermodynamic consistency and agreement with the experimental data (Chou and Vannice, 1987c). A model was later proposed for benzene hydrogenation on supported Pd catalysts, which involved assumptions similar to those of Chou and Vannice (1987c), but included some additional simplifications such as: (1) addition of the first H-atom as the rate-determining step; (2) surface

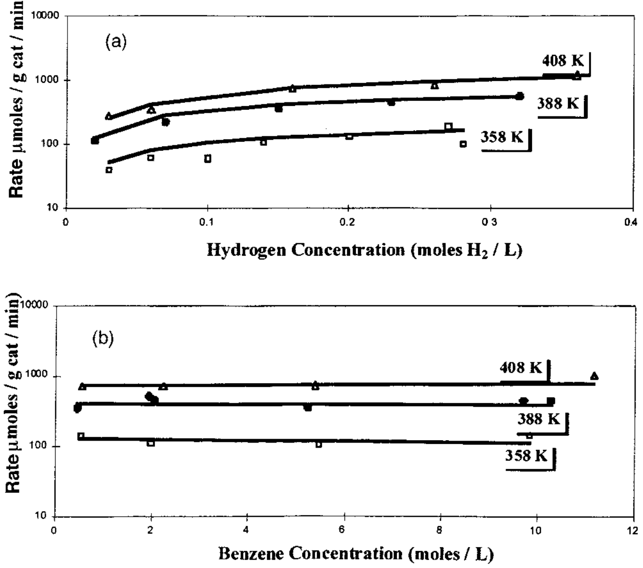

Figure 6. Variation of hydrogenation rate of benzene with: (a) liquid-phase H_2 concentration (open symbols); (b) benzene concentration (open symbols).

Fit of kinetic model (Eq. 5) to experimental data for reaction over 1.20% $Pd/\eta\text{-}Al_2O_3$ is shown by solid lines.

coverage of the dehydrogenated species is much greater than that of benzene; and (3) one hydrogen-deficient species dominates (Lin and Vannice, 1993b). This model again provided thermodynamic consistency and fit the experimental data well. The model proposed by Chou and Vannice was later effectively utilized to describe the vapor-phase hydrogenation of ethyl benzene (Smeds et al., 1995), and the validity of the model proposed for Pt (Lin and Vannice, 1993b) has received support from Tetenyi (1994), based on his isotopic labeling studies. Other evidence to support this latter model has been presented and discussed elsewhere (Lin and Vannice, 1993b; Poondi and Vannice, 1996).

In this study, the rationale behind the previous models was extended to include liquid-phase benzene hydrogenation. The model can be described by the following sequence of steps:

$$\mathrm{Bz}+\mathrm{S}_1 \overset{K_{\mathrm{Bz}}}{\rightleftharpoons} \mathrm{Bz}-\mathrm{S}_1$$

$$3[\mathrm{H}_2+2\mathrm{S}_2 \overset{K_{\mathrm{H}}}{\rightleftharpoons} 2\mathrm{H}-\mathrm{S}_2]$$

$$\mathrm{Bz}-\mathrm{S}_1+\mathrm{H}-\mathrm{S}_2 \xrightarrow{k} \mathrm{BzH}-\mathrm{S}_1+\mathrm{S}_2 \quad (\mathrm{RDS})$$

$$\mathrm{Bz}-\mathrm{S}_1+\mathrm{S}_2 \overset{K_{\mathrm{D}_1}}{\rightleftharpoons} \mathrm{D}_1-\mathrm{S}_1+\mathrm{H}-\mathrm{S}_2$$

$$\mathrm{BzHS}_1+5\mathrm{H}-\mathrm{S}_2 \overset{K}{\rightleftharpoons} \mathrm{C}_6\mathrm{H}_{12}+\mathrm{S}_1+5\mathrm{S}_2$$

where D_1 is a dehydrogenated benzene species. Assuming addition of the first H-atom to break the resonance structure to be the rate determining step, the reaction rate is described by

$$r_{\mathrm{Bz}} = k\Theta_{\mathrm{Bz}}\Theta_{\mathrm{H}}, \tag{1}$$

where Θ_{Bz} and Θ_{H} are the fractional surface coverages of benzene and hydrogen on sites S_1 and S_2, respectively, and k is the rate constant for the addition of the first H atom to the benzene ring. The assumption of quasi-equilibrated H_2 adsorption on S_2 sites yields the following expressions for surface coverage of H_2 and benzene:

$$\Theta_{\mathrm{H}} = K_{\mathrm{H}}^{1/2}C_{\mathrm{H}_2}^{1/2}\Theta_{\mathrm{S}_2} = \frac{K_{\mathrm{H}}^{1/2}C_{\mathrm{H}_2}^{1/2}}{1+K_{\mathrm{H}}^{1/2}C_{\mathrm{H}_2}^{1/2}}, \tag{2}$$

where C_{H_2} is the liquid-phase concentration of H_2. Quasi-equilibrated benzene adsorption on S_1 sites gives:

$$\Theta_{\mathrm{Bz}} = K_{\mathrm{Bz}}C_{\mathrm{Bz}}\Theta_{\mathrm{S}_1}. \tag{3}$$

Assuming only adsorbed benzene and one H-deficient benzene species are dominant on the surface, the site balance on sites of type S_1 yields

$$\Theta_{\mathrm{S}_1} = \frac{1}{1+\dfrac{K_{\mathrm{D}}K_{\mathrm{Bz}}C_{\mathrm{Bz}}}{K_{\mathrm{H}}^{1/2}C_{\mathrm{H}_2}^{1/2}}+K_{\mathrm{Bz}}C_{\mathrm{Bz}}}, \tag{4}$$

where C_{Bz} is the liquid-phase benzene concentration. The second term in the denominator of Eq. 4 arises from the H-deficient surface species, assumed to be a phenyl species, which is in equilibrium with adsorbed benzene and hydrogen. Combining the preceding equations and rearranging yields the following rate expression:

$$r_{\mathrm{Bz}} = \frac{(kK_{\mathrm{H}}K_{\mathrm{Bz}})C_{\mathrm{Bz}}C_{\mathrm{H}_2}}{\left[1+(K_{\mathrm{H}}^{1/2})C_{\mathrm{H}_2}^{1/2}\right]\left[(K_{\mathrm{H}}^{1/2})C_{\mathrm{H}_2}^{1/2}+(K_{\mathrm{Bz}}K_{\mathrm{H}}^{1/2})C_{\mathrm{Bz}}C_{\mathrm{H}_2}^{1/2}+(K_{\mathrm{D}}K_{\mathrm{Bz}})C_{\mathrm{Bz}}\right]}, \tag{5}$$

where K_{D} is the equilibrium constant for the dehydrogenation reaction that forms the H-deficient phenyl species on the surface. The temperature dependence of the equilibrium constants and the rate constant is expressed as follows:

$$k = A_0\exp\left(-\frac{E_a}{RT}\right)$$

$$K_i = \exp\left(\frac{\Delta S_{\mathrm{ad}}^0}{R}-\frac{\Delta H_{\mathrm{ad}}^0}{RT}\right), \tag{6}$$

where A_0, E_a, ΔH_{ad}^0, ΔS_{ad}^0 are the preexponential factor, activation energy, standard enthalpy of adsorption, and standard entropy of adsorption, respectively. Kinetic modeling was performed using the Microsoft Excel Solver Routine, and the rate data at each of the three temperatures (358 K, 388

K, 408 K) was fitted separately using four adjustable parameters. Local minima were avoided by using widely varied initial guesses and observing that the final parameters converged to similar values.

Prior to rationalizing various aspects of the preceding model, it is instructive to consider whether the liquid-phase hydrogen concentration or the H_2 partial pressure is the preferred choice in the rate expression. Madon et al. (1978) reported that for liquid-phase hydrogenation of cyclohexene on supported Pt catalysts, the H_2 concentration is the better choice in the rate expression. Their results clearly showed that when the reaction was conducted in different solvents, free of all transport limitations, and the partial pressure of H_2 was used in the rate expression, the resulting apparent rate constant exhibited a 3-fold variation with solvent. However, when the liquid-phase H_2 concentration was utilized in the rate expression, the resulting rate constants were essentially independent of the solvent and fell within 10% of an average value (Madon et al., 1978). Their results are listed in Table 3. Similar results were also observed by Boudart and Sajkowski (1991) during liquid-phase hydrogenation of cyclohexene over supported Rh catalysts. The solvent-independent rate constant was shown to be the intrinsic reaction rate constant multiplied by the ratio of the activity coefficient of H_2 in the liquid phase to that of H_2 in the transition state just prior to dissociative adsorption, which was proposed as the rate-determining step (Madon et al., 1978; Boudart and Dejega-Mariadassou, 1984).

Madon et al. (1978) examined the effect of H_2 solubility on liquid-phase reactions by considering the case where H_2 in the gas phase was in equilibrium with H_2 in the liquid phase, which was also in equilibrium with the transition state of H_2 prior to dissociative adsorption. They proposed that the observed rate was proportional to the concentration of the transition state ($r \alpha C_t$). In the present study, H_2 in the gas phase, liquid phase, and adsorbed state is assumed to be quasi equilibrated, and the observed rate is proportional to the coverage of adsorbed hydrogen ($r \alpha \Theta_H$). In both cases the reactive hydrogen species in the rate-determining step is equilibrated with H_2 in the gas phase; therefore, an analysis similar to that performed by Madon et al. (1978) should also be valid for the present case and can be extended to include quasi-equilibrated hydrogen adsorption, and thus describe the surface coverage of hydrogen during liquid-phase hydrogenation.

The sequence of elementary steps that describes the dissociative adsorption of hydrogen in a three-phase system consisting of gas-phase hydrogen, liquid-phase solvent, and solid catalyst includes:

$$H_2(g) \rightleftharpoons H_2(l) \tag{7}$$

$$H_2(l) + 2S_2 \rightleftharpoons 2H - S_2, \tag{8}$$

where the first step represents the vapor−liquid equilibrium, while the second step represents the equilibrium for dissociative adsorption of hydrogen on surface sites, S_2. The equilibrium for the second step in the adsorption process (Eq. 8) can be formally written as

$$\sum \nu_i \mu_i = 2\mu_{HS} - \mu^L_{H_2} - 2\mu_{S_2} = 0, \tag{9}$$

where the subscripts HS and S refer to adsorbed hydrogen and the vacant site, respectively. The constraint for vapor-liquid equilibrium requires the chemical potentials of the two phases to be equal, that is,

$$\begin{aligned} \mu^G_{H_2} &= \mu^L_{H_2} \\ \mu^G_{H_2} &= \mu^{O,G}_{H_2} + RT\ln\left(P_{H_2}\right) \\ \mu^L_{H_2} &= \mu^{O,L}_{H_2} + RT\ln\left(C_{H_2}\right) \end{aligned} \tag{10}$$

The standard state for the chemical potential in the gas phase is chosen as 1 atm hydrogen, while that for the liquid phase is chosen as infinitely dilute hydrogen at unit fugacity. The chemical potentials of the adsorbed hydrogen and the vacant site are defined using the conventional Langmuirian approach, which disregards interactions among the adsorbed species ($\gamma_i = 1$). This can be formally stated as:

$$\begin{aligned} \mu_{HS} &= \mu^O_{HS} + RT\ln(\Theta_{HS}) \\ \mu_S &= \mu^O_S + RT\ln(\Theta_S), \end{aligned} \tag{11}$$

and the standard state is defined for a condition of infinitely dilute hydrogen in the liquid phase. Substituting Eqs. 10 and 11 into Eq. 9, the following expression is obtained

$$\frac{\Theta_{HS}}{\Theta_S} = P_H^{1/2}\exp\left(\frac{\mu^{O,G}_{H_2} + 2\mu^O_S - 2\mu^O_{HS}}{2\,RT}\right). \tag{12}$$

Assuming no significant solvent adsorption and utilizing the site balance ($\Theta_{HS} + \Theta_S = 1$), the expression for surface coverage of hydrogen becomes:

$$\Theta_{HS} = \frac{\left(K_H|_{solv}\right)^{1/2} P^{1/2}_{H_2}}{1 + \left(K_H|_{solv}\right)^{1/2} P^{1/2}_{H_2}}, \tag{13}$$

where $K_H|_{solv}$ is the equilibrium constant for the sum of steps 7 and 8. The square root of $K_H|_{solv}$ is

$$\left(K_H|_{solv}\right)^{1/2} = \exp\left(\frac{\mu^{O,G}_{H_2} + 2\mu^O_S|_{solv} - 2\mu^O_{HS}|_{solv}}{2\,RT}\right). \tag{14}$$

Table 3. Rate Constants for Cyclohexene Hydrogenation Evaluated Using H_2 Partial Pressure or Liquid-Phase Concentration

Solvent	$k\ (P_{H_2}) \times 10{,}000$	$k'\ (C_{H_2}) \times 10{,}000$
Cyclohexane	3.6	3.6
n-Heptane	5.3	4.3
p-Dioxane	2.0	4.2
Ethyl acetate	4.3	4.5
Methanol	3.3	3.9
Benzene	2.9	3.7
Cyclohexene	3.5	3.9

Source: Madon et al. (1978).

The standard states for the vacant sites and the adsorbed hydrogen are not solvent independent, and thus $K_H|_{\mathrm{solv}}$ may change, depending on the nature of the solvent. Therefore, it is desirable to switch to standard states that will yield an intrinsic solvent-independent adsorption equilibrium constant, K_H. The standard state for hydrogen in the gas phase is 1 atm and independent of the solvent. However, the standard-state chemical potential for the vacant site and the adsorbed hydrogen, defined at infinitely dilute hydrogen in the liquid phase, can be influenced by the solvent. Therefore, the standard states of the vacant site and the adsorbed hydrogen are redefined as follows:

$$\mu_S^O|_{\mathrm{solv}} = \mu_S^O|_{\mathrm{no\,solv}} + C_1$$

$$\mu_{HS}^O|_{\mathrm{solv}} = \mu_{HS}^O|_{\mathrm{no\,solv}} + C_2, \qquad (15)$$

where C_1 and C_2 are constants that account for the effect of solvent on the chemical potential of the vacant sites and adsorbed hydrogen. The standard-state chemical potential of the vacant site and adsorbed state of hydrogen in the absence of solvent (denoted by the subscript "no solv") can now be redefined as that referred to 1 atm hydrogen in the gas phase, and it is solvent independent. Substituting the preceding two expressions into the exponential in Eq. 14, one obtains:

$$K_H^{1/2}|_{\mathrm{solv}} = \exp\left(\frac{\frac{1}{2}\mu_{H_2}^{O,G} + \mu_S^O|_{\mathrm{no\,solv}} - \mu_{HS}^O|_{\mathrm{no\,solv}}}{RT}\right)$$

$$* \exp\left(\frac{\mu_S^O|_{\mathrm{solv}} - \mu_S^O|_{\mathrm{no\,solv}}}{RT} - \frac{\mu_{HS}^O|_{\mathrm{solv}} - \mu_{HS}^O|_{\mathrm{no\,solv}}}{RT}\right). \qquad (16)$$

The first exponential is the intrinsic adsorption equilibrium constant for hydrogen that is independent of the solvent, while the second exponential accounts for the effect of solvent on the adsorption equilibrium constant of hydrogen. Therefore, the following general expression for the fractional surface coverage of hydrogen is obtained from Eq. 13:

$$\Theta_{HS} = \frac{\alpha K_H^{1/2} P_{H_2}^{1/2}}{1 + \alpha K_H^{1/2} P_{H_2}^{1/2}}, \qquad (17)$$

where K_H is the intrinsic adsorption equilibrium constant independent of the solvent, while α characterizes the effect of the solvent on the adsorption equilibrium constant and is defined as follows:

$$\alpha = \exp\left(\frac{\mu_S^O|_{\mathrm{solv}} - \mu_S^O|_{\mathrm{no\,solv}}}{RT} - \frac{\mu_{HS}^O|_{\mathrm{solv}} - \mu_{HS}^O|_{\mathrm{no\,solv}}}{RT}\right). \qquad (18)$$

For the case where the effect of solvent on the standard-state chemical potential is zero or negligible, $\alpha = 1$, and the equation for the surface coverage of hydrogen (Eq. 17) simplifies to

$$\Theta_{HS} = \frac{K_H^{1/2} P_{H_2}^{1/2}}{1 + K_H^{1/2} P_{H_2}^{1/2}}. \qquad (19)$$

In this case the solvent merely serves as a transparent barrier for H_2 availability to the surface, and use of the hydrogen partial pressure allows direct evaluation of the adsorption equilibrium constant. In addition, the fractional surface coverage of hydrogen is constant at a given partial pressure of hydrogen, independent of the solvent. This case is expected to be rare, and indeed experimental data point to the fact solvent effects are prevalent even for seemingly ideal solvents such as *n*-hexane and *n*-heptane (Madon et al., 1978; Rajadhyaksha and Karwa, 1986).

If solvent effects play an important role, then α is not unity. The solvent effect on the standard state of the adsorbed phase can be further expanded assuming an additive relationship for standard-state chemical potentials of the adsorbed hydrogen as follows:

$$\mu_{HS}^O = \mu_H^O + \mu_S^O + C_3, \qquad (20)$$

where C_3 represents the contribution of the solvent-independent interaction between the hydrogen atom and adsorption site. The preceding additive property holds in the presence and absence of solvent and therefore the following expressions are obtained:

$$\mu_{HS}^O|_{\mathrm{solv}} = \mu_H^O|_{\mathrm{solv}} + \mu_S^O|_{\mathrm{solv}} + C_3$$

$$\mu_{HS}^O|_{\mathrm{no\,solv}} = \mu_H^O|_{\mathrm{no\,solv}} + \mu_S^O|_{\mathrm{no\,solv}} + C_3. \qquad (21)$$

Substitution of Eq. 21 into Eq.18 yields the following expression for α:

$$\alpha = \exp\left(\frac{\mu_H^O|_{\mathrm{no\,solv}} - \mu_H^O|_{\mathrm{solv}}}{RT}\right). \qquad (22)$$

The standard-state chemical potential of the hydrogen atom can be related to that of the hydrogen molecule by assuming the relationship below:

$$\mu_{H_2}^O|_{\mathrm{solv}} = 2\mu_H^O|_{\mathrm{solv}} + C_4$$

$$\mu_{H_2}^O|_{\mathrm{no\,solv}} = 2\mu_H^O|_{\mathrm{no\,solv}} + C_4, \qquad (23)$$

where C_4 represents the contribution of a solvent-independent interaction between the two hydrogen atoms in a hydrogen molecule. Substitution of Eq. 23 into Eq. 22 yields the following expression for α:

$$\alpha = \exp\left(\frac{\mu_{H_2}^O|_{\mathrm{no\,solv}} - \mu_{H_2}^O|_{\mathrm{solv}}}{2\,RT}\right). \qquad (24)$$

Greater insight into the physical meaning of α is obtained by equating chemical potentials of gas- and liquid-phase hydrogen (Eq. 10) to obtain:

$$\mu_{H_2}^{O,G} + RT\ln\left(P_{H_2}\right) = \mu_{H_2}^{O,L} + RT\ln\left(C_{H_2}\right)$$

$$\mu_{H_2}^{O,L} - \mu_{H_2}^{O,G} = RT\ln\left(\frac{P_{H_2}}{C_{H_2}}\right) = RT\ln(\mathrm{H}). \qquad (25)$$

Realizing that

$$\mu^{O}_{\mathrm{H}_2}|_{\text{no solv}} = \mu^{O,G}_{\mathrm{H}_2}$$

$$\mu^{O}_{\mathrm{H}_2}|_{\text{solv}} = \mu^{O,L}_{\mathrm{H}_2} \tag{26}$$

Eqs. 21 and 20 can be combined to yield

$$\alpha = H^{-1/2}, \tag{27}$$

where H is the constant in Henry's law. Therefore, for the case where the solvent can affect the metal surface, the fractional coverage of hydrogen can be obtained by substituting Eq. 23 into Eq. 17, yielding

$$\Theta_{\mathrm{HS}} = \frac{H^{-1/2}K_{\mathrm{H}}^{1/2}P_{\mathrm{H}_2}^{1/2}}{1+H^{-1/2}K_{\mathrm{H}}^{1/2}P_{\mathrm{H}_2}^{1/2}} = \Theta_{\mathrm{H}}. \tag{28}$$

Thus, if partial pressure is utilized and a solvent effect is significant, the intrinsic adsorption equilibrium constant is coupled with the Henry's law constant, yielding an apparent adsorption equilibrium constant that can change with solvent composition. However, if Henry's law is substituted into this expression, that is, $P_{\mathrm{H}_2} = H * C_{\mathrm{H}_2}$, the resulting equation for surface coverage of hydrogen is now

$$\Theta_{\mathrm{HS}} = \frac{K_{\mathrm{H}}^{1/2}C_{\mathrm{H}_2}^{1/2}}{1+K_{\mathrm{H}}^{1/2}C_{\mathrm{H}_2}^{1/2}} = \Theta_{\mathrm{H}}. \tag{29}$$

Therefore, in the presence of solvent effects, an intrinsic adsorption equilibrium constant free of solvent effects can still be extracted if the liquid-phase hydrogen concentration is used in place of hydrogen partial pressure. Furthermore, in the presence of solvent effects, increasing the hydrogen solubility at a constant partial pressure of hydrogen can increase the surface coverage of hydrogen. The results from the preceding derivation are analogous to those derived by Madon et al. (1978) for cyclohexane hydrogenation over Pt/SiO$_2$ in various solvents.

Special care must be taken to distinguish between different types of solvent effects. As stated previously, solvent effects can be induced in numerous ways, including competitive adsorption with the reactants and products, as well as interaction of the organic reactants with the electronic environment of the solvent as characterized by the dielectric constant. The complete treatment of these cases on a theoretical basis is beyond the scope of the present study. The solvent effect that is related to the preceding analysis pertains only to the influence of the solvent on the hydrogen dissolved in the liquid phase. The preceding equations indicate that in the absence of solvent effects, the hydrogen partial pressure is best suited for the rate expression yielding solvent-independent adsorption equilibrium constants, and the surface coverage of hydrogen is constant at a given partial pressure of hydrogen, independent of the solvent. In the presence of solvent effects, use of liquid-phase hydrogen concentration in the surface-coverage expression, and hence the rate expression, is preferred because it yields an intrinsic adsorption equilibrium constant independent of solvent. Furthermore the fractional surface coverage of hydrogen can increase with increasing hydrogen solubility at a constant partial pressure of hydrogen, even when the assumption of quasi-equilibrated adsorption of hydrogen is valid.

The question then arises as to whether liquid-phase hydrogen concentration or partial pressure of hydrogen in the gas phase should be used in the rate expression. Insight into this question was gained through the work of Madon et al. (1978) and Boudart and Sajkowski (1991), who showed that, even for a nonpolar and seemingly ideal solvent such as *n*-heptane, the interaction of the solvent with the hydrogen molecule is significant during liquid-phase hydrogenation of cyclohexene. Their results show that a solvent-independent rate constant is obtained when liquid-phase hydrogen concentration is explicitly used in the rate expression in place of partial pressure of hydrogen. Therefore, since a similar solvent was used in this study, the liquid-phase hydrogen concentration, obtained from Henry's law, was used in the rate expression. The Henry's law constant was derived from the SRK-EOS (Soave-Redlich-Kwong equation of state) with a temperature-dependent k_{ij} parameter (Moysan et al., 1983). Figure 7 shows a comparison between the calculated values and the experimental data reported in the literature for pure benzene and *n*-hexane. The Henry's law constant for a mixture of benzene and *n*-hexane was evaluated using regular solution theory (Prausnitz et al., 1986). The effect of cyclohexane was ignored, since the reaction was conducted in a differential mode where cyclohexane concentration is low and its effect on H$_2$ solubility can be considered negligible. It is important to note that the pure-component Henry's constant for hexane and benzene differ 3-fold. This has important consequences for the reaction-rate expression, since the liquid-phase concentration of H$_2$ changes significantly as the benzene concentration changes in the reaction mixture. Therefore, the liquid-phase concentration of hydrogen was explicitly used in the rate expression to account for solvent effects [as described in

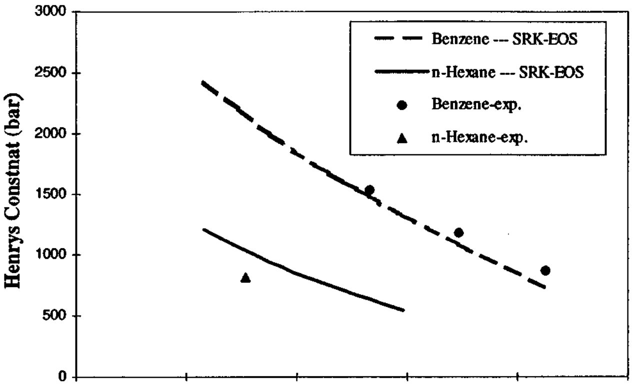

Figure 7. Liquid-phase H$_2$ concentration evaluated using the Soave-Redlich-Kwong equation of state.

Lines are Henrys constant predicted from the SRK-EOS, and points represent values obtained from the literature (Moysan et al., 1983).

the previous derivation and analogous to the observations by Madon et al. (1978) for cyclohexene hydrogenation].

The fit of the reaction rate expression to experimental data is displayed in Figure 6. For a model to be acceptable it must not only show a good fit to experimental data, but it must also explain other observations and exhibit thermodynamic consistency. In this respect, the main features of the model will be addressed primarily in the context of vapor-phase benzene hydrogenation studies. *In-situ* catalyst characterization during liquid-phase reactions is difficult, and therefore the literature providing information about the state of the catalyst under these reaction conditions is scant.

Dissociative adsorption of H_2 on Group VIII metals has been well documented in the literature (Munn and Clary, 1997) and has been successfully invoked in numerous kinetic studies of vapor-phase benzene hydrogenation (van Meerten and Coenen, 1977; Chou and Vannice, 1987c; Lin and Vannice, 1993b). In addition, magnetization measurements by van Meerten et al. (1977) indicated that dissociatively adsorbed hydrogen was the active species for benzene hydrogenation on a Ni/SiO_2 catalyst.

Benzene adsorption on Group VIII metals can occur via an adsorption state where the ring lies parallel to the surface (Prasad et al., 1983; Basset et al., 1995; Stair and Somorjai, 1977; Surman et al., 1983, 1987; Fajarde et al., 1996; Abon et al., 1985; van Meerten et al., 1979), as well as one where the ring may be distorted or inclined to the surface (Prasad et al., 1983; Stair and Somorjai, 1977; van Meerten et al., 1979). For benzene adsorption on the Pt(111) surface, Stair and Somorjai (1977) determined the surface carbon concentration by Auger measurements and found the C/Pt ratio to be much higher than expected if benzene were adsorbed in a π-mode alone. Van Meerten et al. (1979) used statistical thermodynamic arguments to show that the presence of only the associatively π-complex of benzene could not explain the observed isotope effect for the reaction of D_2 with C_6H_6 and H_2 with C_6D_6. A π-complex substitution mechanism yielding a monodehydrogenated benzene ring adsorbed via the σ-mode and an adsorbed H atom better explained the observed isotope effects (van Meerten et al., 1979). It is believed that benzene adsorption occurs through the π-mode with the ring parallel to the surface as well as through a σ-type bonding where the ring may be distorted (Prasad et al., 1983; van Meerten et al., 1979). Prasad et al. (1983) explicitly accounted for both modes of benzene adsorption in developing a model to explain their observed kinetics, and they suggested that benzene adsorbed in the π-mode is the reactive form for hydrogenation, whereas the σ-bonded benzene is inhibitive.

The model proposed earlier for vapor-phase benzene hydrogenation on Pt (Lin and Vannice, 1993b) and extended to Pd in the present study also proposes that some of the adsorbed benzene serves as an inhibitor by occupying adsorption sites as a dehydrogenated phenyl species. Evidence exists that suggests that only a fraction of the adsorbed benzene is hydrogenated to cyclohexene (Mirodatos, 1986). Some of the adsorbed benzene may be dehydrogenated, because Tsai et al. (1982) utilized TPD measurements to show that olefin dehydrogenation reactions occurred on stepped Pt surfaces. Myers et al. (1987) reported evolution of H_2 during their study of benzene decomposition over single-crystal Ni surfaces. Szilagyi's FTIR study of benzene adsorption on Pt/SiO_2 catalysts revealed that several reactions were taking place simultaneously with benzene hydrogenation, including self-hydrogenation, rapid H−D exchange, and dehydrogenation. His results suggest that the carbonaceous deposits on the surface can reversibly take up and release hydrogen without desorbing as cyclohexane (Szilagyi, 1988). It has also been suggested that benzene adsorbed in the π-mode is in equilibrium with benzene adsorbed in the σ-mode, which in turn yields an adsorbed H atom and a monodehydrogenated phenyl species (Moyes and Wells, 1973).

It should be pointed out that much of the work on olefin dehydrogenation has been performed on Pt and Ni surfaces rather than Pd, as utilized in the present study. Orozco and Webb (1983) studied the adsorption and hydrogenation of benzene on supported Pt and Pd catalysts, and their results indicated that while benzene dehydrogenation was observed on the Pt catalyst, no such processes were observed on the Pd catalyst in the presence of hydrogen. However, their results do indicate that dehydrogenation may be taking place in the absence of hydrogen. The authors attributed this to the ability of Pd to absorb hydrogen, thus keeping the metal surface saturated with H and preventing dissociation of the benzene ring (Orozco and Webb, 1983). However, in the case of liquid-phase benzene hydrogenation, the benzene activity at the catalyst surface is much greater than that during vapor-phase studies, and this greater driving force may reduce the ability of Pd to adsorb and absorb hydrogen, thus allowing dehydrogenation of the benzene ring. In vapor-phase studies of benzene hydrogenation over Pd catalysts, Chou and Vannice (1987c) explicitly accounted for dehydrogenation processes to successfully fit the kinetic model to the observed experimental data.

The model set forth in the present study also proposes that H atoms adsorb on different sites than benzene. As before, no studies could be found that examined H_2 adsorption in the presence of liquid-phase benzene; however, numerous vapor-phase studies suggest that in fact benzene and hydrogen adsorb on separate sites. Mirodatos (1986) and Mirodatos et al. (1987) showed that the H coverage on Ni catalysts in the presence of benzene was within 10% of the H coverage in a benzene-free system; thus, benzene blocks few of the H adsorption sites. Van Meerten et al. (1977) utilized magnetization measurements to conclude that for benzene hydrogenation on Ni catalysts, hydrogen and benzene adsorb noncompetitively. Extended Huckel calculations of Myers et al. (1987) show that the most stable site for benzene adsorption was above the 4-fold hollow sites for Ni(100) and above the 3-fold hollow sites for Ni(111) surface. Hydrogen, on the other hand, adsorbs in the 3- and 4-fold hollow sites present on (111) and (100) planes, respectively, present in fcc Group VIII metals (Shustrorovich, 1990). In addition, some of the models examined in the present study that employed competitive adsorption between hydrogen and benzene were discarded because the kinetic constraint that the order with respect to hydrogen approach zero at very high hydrogen pressure was not obeyed (Temkin, 1989). The present model also proposes that addition of the first H atom is the rate-determining step. This is intuitively satisfactory, as one would anticipate that the largest activation barrier should be that for breaking the resonance of the aromatic ring. It has been proposed by some that hy-

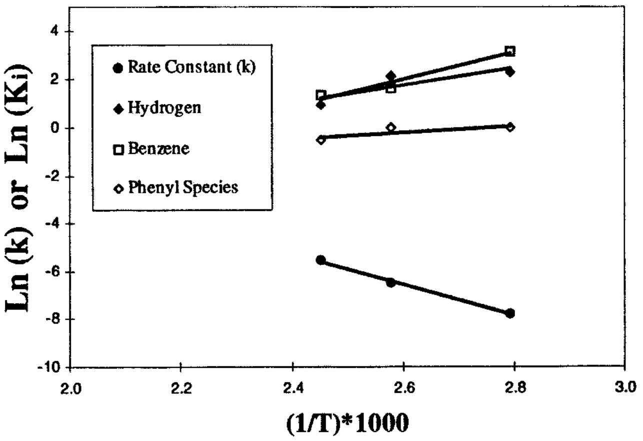

Figure 8. Arrhenius behavior of the adsorption equilibrium constants and rate constants in the reaction rate expression.

drogenation proceeds by the simultaneous addition of two H atoms to the aromatic ring (Mirodatos et al., 1987; Temkin, 1989). While this assumption provided an adequate fit to the present data, it is not preferred, since it requires a less probable 3-body reaction. Radiotracer studies by Derbentsev et al. (1972), Tetenyi (1994), and Tetenyi and Paal (1972) indicated a direct hydrogenation route from benzene to cyclohexane through the addition of H atoms. In addition, they proposed that H atoms are sequentially added to benzene in a 1,3,5-mode (meta-addition of hydrogen atoms) (Derbentsev et al., 1972; Tetenyi and Paal, 1972).

As another check of the model, the thermodynamic consistency of the fitted parameters was investigated. The enthalpy and entropy of adsorption for benzene were obtained from the Arrhenius plots shown in Figure 8, and the standard states were changed to 1 atm in the gas phase. The standard state for ΔH_{Bz} and ΔS_{Bz} was changed from liquid at 1 mol Bz/L to pure gas at 1 atm by following the path shown in Figure 9. ΔH^o, ΔS^o at the standard state of 1 atm in gas phase is related to ΔH, ΔS in the liquid phase at 1 mol/L as follows (Mears and Boudart, 1966):

$$\begin{aligned}\Delta S^o_{\mathrm{Bz}}(1\ \mathrm{atm}) &= \Delta S^o_{\mathrm{Bz}}(1\ \mathrm{M}) + |\Delta S_{\mathrm{mix,Bz}}| - |\Delta S^L_T| \\ &\quad - |\Delta S_{\mathrm{vap,Bz}}| + |\Delta S^G_T| = \Delta S^o_{\mathrm{Bz}}(1\ \mathrm{M}) - 25 \\ \Delta H^o_{\mathrm{Bz}}(1\ \mathrm{atm}) &= \Delta H^o_{\mathrm{Bz}}(1\ \mathrm{M}) - |\Delta H^L_T| - |\Delta H_{\mathrm{vap,Bz}}| + |\Delta H^G_T| \\ &= \Delta H^o_{\mathrm{Bz}}(1\ \mathrm{M}) - 8, \qquad (30)\end{aligned}$$

where the individual terms are defined in the Notation section. A similar change in standard state was also required for the enthalpy and entropy of adsorption of hydrogen. The standard state was changed from 1 mol H_2/L in the liquid phase to 1 atm in the gas phase by the following path, that is, 1 mol/L liquid-phase H_2 at 298 K $\overset{0}{\rightleftharpoons}$ gas-phase H_2 at 298 K $\longrightarrow$ gas-phase H_2, 1 atm and 298 K, which yields the expression below:

$$\begin{aligned}\Delta S^o_{\mathrm{H_2}}(1\ \mathrm{atm}) &= \Delta S^o_{\mathrm{H_2}}(1\ \mathrm{M}) + |\Delta S_{\mathrm{exp,H_2}}| = \Delta S^o_{\mathrm{H_2}}(1\ \mathrm{M}) - 10 \\ \Delta H^o_{\mathrm{H_2}}(1\ \mathrm{atm}) &= \Delta H^o_{\mathrm{H_2}}(1\ \mathrm{M}). \qquad (31)\end{aligned}$$

The enthalpy and entropy of adsorption for benzene and hydrogen are negative as required by thermodynamics, and also are in general agreement with the additional thermodynamic constraints:

$$\begin{aligned}&0 < |\Delta S^o_{ad}| \le S^o_g \\ &10 \le \Delta S^o_{ad} \le 12 - 0.0014(\Delta H^o_{ad}), \qquad (32)\end{aligned}$$

where ΔS^o_{ad}, ΔH^o_{ad} are values for the entropy and enthalpy of adsorption, respectively, and S^o_g is the standard entropy of

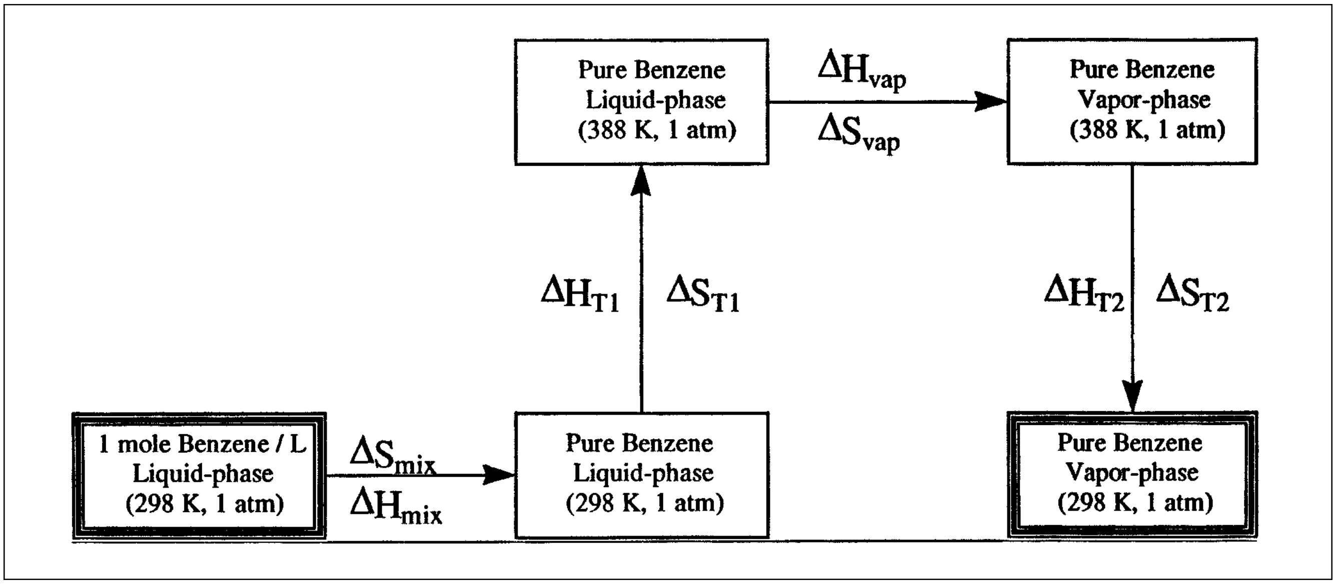

Figure 9. Thermodynamic path followed for changing the standard state for enthalpy and entropy of adsorption of benzene from 1 mol/L in liquid-phase to 1 atm in the vapor phase.

Table 4. Comparison of TOFs, Apparent Activation Energies, and Reaction Orders for Liquid- and Vapor-Phase Studies over Pd/η-Al_2O_3 Catalysts

	Vapor Phase	Liquid Phase
TOF (s^{-1})	0.091*	0.26**
Ea (kcal/mol)	12 †	9 ‡
Order in Bz	0 −0.1†	0 −0.1**
Order in H_2	0.6−0.8†	0.5−0.6**

Source: Chou and Vannice (1987b).

*Evaluated at 413 K, 1 atm H_2 pressure.

**Evaluated at 413 K, 13.6 atm H_2 pressure.

†Evaluated between 373 K and 423 K, 1 atm H_2.

‡Evaluated between 353 K and 473 K, 54 atm H_2.

Table 5. Comparison of Thermodynamic Parameters for Liquid- and Vapor-Phase Studies*

	Vapor Phase		Liquid Phase	
	ΔH^o, E_{act} (kcal/mol)	ΔS^o, ln A (cal/mol/°C)	ΔH^o, E_{act} (kcal/mol)	ΔS^o, ln A (cal/mol/°C)
k	7	14	13	10
K_B	−20	−34	−19	−49
K_H	−2	−15	−7	−25
K_D	−1	−10	−3	−7

*Standard state is 1 atm.

Source: Chou and Vannice (1987c).

the gas. The first constraint is stringent, while the second criteria only represent general guidelines (Boudart et al., 1967; Boudart, 1972; Vannice et al., 1979). The values of absolute entropy for benzene and hydrogen at 298 K are 70 e.u. (entropy unit) and 31 e.u., respectively, which are significantly larger than the changes in entropy of adsorption obtained from the fitted parameters.

The kinetics reported in the present study were obtained under differential reaction conditions shown to be free of all heat and mass-transfer effects, and can therefore be compared to a previous study (Chou and Vannice, 1987c). Table 4 shows a comparison between vapor- and liquid-phase hydrogenation for values of TOF, apparent activation energy, and reaction orders in benzene and hydrogen, and the results reveal that the kinetics for vapor-phase and liquid-phase hydrogenation reactions are similar. It is interesting to note that the TOF for the liquid-phase reaction at 413 K and 13.6 atm H_2 is 0.26 s^{-1} as compared to 0.091 s^{-1} for vapor-phase reaction at 413 K and 1 atm H_2 pressure, that is, a 13-fold increase in hydrogen pressure results in only a 3-fold change in TOF. This may be attributable to the larger thermodynamic activity of benzene that could either alter the concentration of S_2 sites or enhance the concentration of the H-deficient species on the surface or both. It is also worthwhile to mention that the Arrhenius plot of benzene hydrogenation from 358 K to 483 K at 54 atm H_2 pressure does not exhibit an activity maximum in the reaction rate. Activity maxima in Arrhenius plots of vapor-phase studies have been attributed to the compensation caused by an increasing reaction rate constant and a decreasing adsorption-equilibrium constant (thus declining surface concentration) with increasing temperature. The higher thermodynamic activity of benzene at the catalyst surface during liquid-phase hydrogenation does not allow such a sharp decrease in benzene coverage and, if it did, a still higher temperature would be required to create a sharp decrease in the surface coverage of benzene resulting in a decrease in the reaction rate. Odenbrand et al. (1980) did observe an activity maximum at 463 K in their Arrhenius plot at 34 atm hydrogen pressure for the liquid-phase hydrogenation of benzene. However, the authors admit that there was significant leaching of metals from the reactor walls; thus, the possibility exists that leached metals were poisoning the catalyst and may have affected the adsorption properties of benzene on the catalyst surface and allowed an activity maximum.

Table 5 shows a comparison of the fitted thermodynamic parameters (standard state of 1 atm in gas phase) obtained from the vapor- and liquid-phase rate expressions describing kinetics on supported Pd catalysts. Unfortunately, accurate error bars could not be estimated for the fitted parameters in the liquid phase, and therefore quantitative comparisons must be made with caution. Nevertheless, it is interesting to note the common trends between the vapor- and liquid-phase kinetics. The heat of adsorption of benzene is approximately 20 kcal/mol in both the vapor and liquid phases and is in close agreement with the published values of 25 kcal/mol by Yu et al. (1959) for heats of adsorption of benzene on Ni powder at 273 K. The value of −49 e.u. for $\Delta S^o_{ad,Bz}$ reported in the present study is larger than that reported in the vapor-phase study; however, the thermodynamic constraints listed in Eq. 32 are satisfied.

The enthalpy of adsorption for hydrogen in the liquid phase reaction was −7 kcal/mol, which is in reasonable agreement with the vapor-phase study. In addition, the enthalpy of adsorption of hydrogen is similar to the values near −10 kcal/mol for reversible adsorption of hydrogen on supported Pd catalysts (Chou and Vannice, 1987c). Significant evidence exists, in agreement with results from the present study, which suggests that weakly adsorbed hydrogen with heats of adsorption less than 10 kcal/mol is responsible for benzene hydrogenation (Basset et al., 1995; Marecot et al., 1991; Aben et al., 1970). The entropy for adsorption of H_2 was −25 e.u. in the liquid-phase reaction, compared to −15 cal/mol/K in the vapor-phase reaction, and both these values are similar to the value of −20 e.u. reported for hydrogen adsorption on Ni catalysts. Finally, it is worth noting that the values for the enthalpy and entropy of the dehydrogenation reaction are also similar for both the vapor- and liquid-phase reactions.

Summary

Liquid-phase hydrogenation of benzene was studied over Pd/η-Al_2O_3 catalysts in a regime free of heat and mass-transfer limitations. A kinetic model consistent with vapor-phase studies was found to fit these results. The model invokes dissociative adsorption of H_2, noncompetitive adsorption between H_2 and benzene, and addition of the first H atom as the rate-determining step. In addition, a H-deficient phenyl species is proposed to exist on the surface which serves as an inhibitor under reaction conditions. The kinetics of the vapor- and liquid-phase benzene hydrogenation reactions are very similar, and the thermodynamic parameters extracted from the rate expression exhibited thermodynamic consistency and were similar to values reported for vapor-phase studies conducted at 1 atm.

It was shown that in the presence of solvent effects, the fractional surface coverage of hydrogen can increase with increasing hydrogen solubility although the partial pressure of hydrogen remains constant in the gas phase. Furthermore, it is advantageous to utilize liquid-phase hydrogen concentrations in the rate expression, in the presence of solvent effects, so that the intrinsic adsorption equilibrium constant for hydrogen can be extracted. Liquid-phase hydrogen concentration was explicitly utilized in the present study because a solvent effect on the reaction system was anticipated based on the studies of Madon et al. (1978) and Boudart and Sajkowski (1991).

Acknowledgments

The authors thank Dr. J. L. Duda and Dr. R. Nagarajan for fruitful discussions and helpful suggestions regarding thermodynamics analysis of vapor-liquid equilibrium. This study was supported by the DOE Div. of Basic Energy Sciences under Grant No. DE-FE02-84ER13276.

Notation

a_i = thermodynamic activity of species
f_i = fugacity of species i
f_i^o = standard-state fugacity of species i
$\Delta H_{\text{vap,Bz}}$ = enthalpy of vaporization of benzene at 388 K
ΔH_T^G = enthalpy change for decreasing temperature of vapor-phase benzene from 388 to 298 K
ΔH_T^L = enthalpy change in increasing temperature of liquid-phase benzene from 298 to 388 K
$\Delta S_{\text{exp},H_2}$ = entropy change on expansion of H_2 from pressure required to obtain 1 M liquid-phase concentration to 1 atm in the gas phase
$\Delta S^z_{\text{mix,Bz}}$ = entropy change for benzene upon changing standard state from 1 mol/L in the reaction mixture to pure gas at 1 atm
$\Delta S_{\text{vap,Bz}}$ = entropy of vaporization of benzene at 388 K
ΔS_T^G = entropy change for decreasing temperature of vapor-phase benzene from 388 to 298 K
$\Delta S_T^{L,\text{Bz}}$ = entropy change for increasing temperature of liquid-phase benzene from 298 to 388 K
ν_i = stoichiometric coefficient for species i
μ_i = chemical potential of species i
μ_i^o = standard-state chemical potential of species i
γ_I = activity coefficient of species I

Literature Cited

Aben, P. C., J. C. Platteeuw, and B. Stouthamer, "The Hydrogenation of Benzene over Supported Platinum, Palladium, and Nickel Catalysts," *Recl. Trav. Chim. Pays-Bas. Belg.*, **89**, 449 (1970).

Abon, M., J. C. Bertolini, and B. J. Massardier, "Adsorption States of Benzene and Toluene on Pt(111): A Vibrational EELS, $\Delta\phi$, AES, and TDS Study," *Surface Sci.*, **162**, 395 (1985).

Augustine, R. L., "The Stereochemistry of Hydrogenation of α-β Unsaturated Ketones," *Adv. Catal.*, **25**, 56 (1976).

Augustine, R. L., and P. Techasauvapak, "Heterogeneous Catalysis in Organic Synthesis. Part 9: Specific Site Solvent Effects in Catalytic Hydrogenation," *J. Mol. Catal.*, **87**, 95 (1994).

Basset, J. M., G. Dalmai-Imelik, M. Primet, and R. Mutin, "A Study of Benzene Hydrogenation and Identification of the Adsorbed Species with Pt/Al_2O_3 Catalysts," *J. Catal.*, **37**, 22 (1995).

Boudart, M., D. E. Mears, and M. A. Vannice, "Kinetics of Heterogeneous Catalytic Reactions," *Ind. Chim. Belge*, **32**, 281 (1967).

Boudart, M., "Two-Step Catalytic Reactions," *AIChE J.*, **18**, 465 (1972).

Boudart, M., and G. Djega-Mariadassou, *Kinetics of Heterogeneous Catalytic Reactions*, Chap. 5, Princeton Univ. Press, Princeton, NJ (1984).

Boudart, M., and D. J. Sajkowski, "Catalytic Hydrogenation of Cyclohexene: Liquid-Phase Reaction on Rhodium," *Faraday Discuss.*, **92**, 57 (1991).

Chou, P., and M. A. Vannice, "Calorimetric Heat of Adsorption Measurements on Palladium: 1. Influence of Crystallite Size and Support on Hydrogen Adsorption," *J. Catal.*, **104**, 1 (1987a).

Chou, P., and M. A. Vannice, "Benzene Hydrogenation over Supported and Unsupported Palladium: 1. Kinetic Behavior," *J. Catal.*, **107**, 129 (1987b).

Chou, P., and M. A. Vannice, "Benzene Hydrogenation over Supported and Unsupported Palladium: 2. Reaction Model," *J. Catal.*, **107**, 140 (1987c).

Derbentsev, Y. I., Z. Paal, and P. Tetenyi, "Investigation on the Mechanism of Benzene Hydrogenation: A Radiotracer Study," *Z. Phys. Chem. Neue Folge.*, **80**, 51 (1972).

Eckert, C. A., C. K. Hsieh, and J. R. McCabe, "Molecular Thermodynamics for Chemical Reaction Design," *AIChE J.*, **20**, 20 (1974).

Fajarde, F., J.-F. Tempere, G. Djega-Mariadassou, and G. Blanchard, "Benzene Hydrogenation as a Tool for the Determination of the Percentage of Metal Exposed on Low Loaded Ceria Supported Rh Catalysts," *J. Catal.*, **163**, 77 (1996).

Hancock, E. G., *Benzene and Its Derivatives*, Wiley, New York (1975).

Konyukhov, V. Y., S. D. Tret'yakov, A. G. Zyyskin, V. V. Kul'kova, and M. I. Temkin, "Kinetics of Liquid-Phase Hydrogenation of Benzene on Palladium Catalyst and Hydrogenation of Toluene on Palladium and Platinum Catalysts," *Kinet. Catal.*, **28**, 360 (1987).

Lin, S. D., and M. A. Vannice, "Hydrogenation of Aromatic Hydrocarbons over Supported Pt Catalysts: 1. Benzene Hydrogenation," *J. Catal.*, **143**, 539 (1993a).

Lin, S. D., and M. A. Vannice, "Hydrogenation of Aromatic Hydrocarbons over Supported Pt Catalysts: 3. Reaction Models for Metal Surfaces and Acidic Sites on Oxide Supports," *J. Catal.*, **143**, 563 (1993b).

Madon, R. J., J. P. O'Connell, and M. Boudart, "Catalytic Hydrogenation of Cyclohexene. II: Liquid-Phase Reaction on Supported Platinum in a Gradientless Slurry Reactor," *AIChE J.*, **24**, 904 (1978).

Madon, R. J., and M. Boudart, "Experimental Criterion for the Absence of Artifacts in the Measurement of Rates of Heterogeneous Catalytic Reactions," *Ind. Eng. Chem. Fundam.*, **21**, 438 (1982).

Marecot, P. E., J. M. Paraiso, J. M. Dumas, and J. Barbier, "Benzene Hydrogenation on Nickel Catalysts. Role of Weakly-Bound Hydrogen," *Appl. Catal.*, **74**, 261 (1991).

Mears, D. E., and M. Boudart, "The Dehydrogenation of Isopropanol on Catalysts Prepared by Sodium Borohydride Reduction," *AIChE J.*, **12**, 313 (1966).

Mirodatos, C., "Benzene Hydrogenation: An Isotopic Transient Study," *J. Phys. Chem.*, **90**, 481 (1986).

Mirodatos, C., J. A. Dalmon, and G. A. Martin, "Steady-State and Isotopic Transient Kinetics of Benzene Hydrogenation on Ni Catalysts," *J. Catal.*, **105**, 405 (1987).

Moysan, J. M., M. J. Huron, H. Paradowski, and J. Vidal, "Prediction of the Solubility of Hydrogen in Hydrocarbon Solvents through Cubic Equations of State," *Chem. Eng. Sci.*, **38**, 1085 (1983).

Moyes, R. B., and P. B. Wells, "The Chemisorption of Benzene," *Adv. Catal.*, **23**, 121 (1973).

Munn, N. S., and D. C. Clary, "Subsurface Effects in the Dissociation of H_2 on Pd(III)," *Chem. Phys. Lett.*, **266**, 437 (1997).

Myers, A. K., G. R. Schobs, and J. B. Benziger, "Comparison of Benzene Adsorption on Ni(111) and Ni(100)," *J. Phys. Chem.*, **91**, 2230 (1987).

Nagahara, H., M. Ono, M. Konishi, and P. Fukuoka, "Partial Hydrogenation of Benzene to Cyclohexene," *Appl. Surf. Sci.*, **121/122**, 448 (1997).

Odenbrand, C. U. I., and S. T. Lundin, "Hydrogenation of Benzene to Cyclohexene on a Ruthenium Catalyst: Influence of Some Reaction Parameters," *J. Chem. Tech. Biotechnol.*, **30**, 677 (1980).

Orozco, J. M., and G. Webb, "The Adsorption and Hydrogenation of Benzene and Toluene on Alumina- and Silica-Supported Palladium and Platinum Catalysts," *Appl. Catal.*, **6**, 67 (1983).

Palmer, M. B., and M. A. Vannice, "The Effect of Preparation Variables on the Dispersion of Supported Platinum Catalysts," *J. Chem. Tech. Biotechnol.*, **30**, 205 (1980).

Poondi, D. P., and M. A. Vannice, "Competitive Hydrogenation of

Benzene and Toluene on Palladium and Platinum Catalysts,'' *J. Catal.*, **161**, 742 (1996).

Prasad, K. H. V., K. B. S. Prasad, M. M. Mallikarjunan, and R. Vaidyeswaran, ''Self-Poisoning and Rate Multiplicity in Hydrogenation of Benzene,'' *J. Catal.*, **84**, 65 (1983).

Prausnitz, J. M., R. N. Lichtenthaler, and E. G. de Azevedo, *Molecular Thermodynamics of Fluid-Phase Equilibria*, Chap. 2, Prentice Hall, Englewood Cliffs, NJ (1986).

Rajadhyaksha, R. A., and S. L. Karwa, ''Solvent Effects in Catalytic Hydrogenation,'' *Chem. Eng. Sci.*, **41**, 1765 (1986).

Shustrorovich, E., ''The Bond-Order Conservation Approach to Chemisorption and Heterogeneous Catalysis: Applications and Implications,'' *Adv. Catal.*, **37**, 101 (1990).

Smeds, S., D. Murzin, and T. Salmi, ''Kinetics of Ethyl Benzene Hydrogenation on Ni/Al_2O_3,'' *Appl. Catal., A: General*, **125**, 271 (1995).

Stair, P. C., and G. A. Somorjai, ''The Adsorption of Benzene on the Pt(111) Surface Studied by Low-Energy Electron Diffraction Intensity Measurements and Quantitative Auger Electron Spectroscopy,'' *J. Chem. Phys.*, **67**, 4361 (1977).

Struijk, J., M. d'Angremond, W. J. M. Lucas-de-Regt, and J. J. F. Scholten, ''Partial Liquid Phase Hydrogenation of Benzene to Cyclohexene over Ruthenium Catalysts in the Presence of an Aqueous Salt Solution: I. Preparation, Characterization of the Catalyst and Study of a Number of Process Variables,'' *Appl. Catal., A: General*, **83**, 263 (1992a).

Struijk, J., R. Moene, T. van der Kamp, and J. J. F. Scholten, ''Partial Liquid Phase Hydrogenation of Benzene to Cyclohexene over Ruthenium Catalysts in the Presence of an Aqueous Salt Solution: II. Influence of Various Salts on the Performance of the Catalyst,'' *Appl. Catal., A: General*, **89**, 77 (1992b).

Struijk, J., and J. J. F. Scholten, ''Selectivity to Cyclohexenes in the Liquid-Phase Hydrogenation of Benzene and Toluene over Ruthenium Catalysts, As Influenced by Reaction Modifiers,'' *Appl. Catal., A: General*, **82**, 277 (1992).

Surman, M., S. R. Bare, P. Hofmann, and D. A. King, ''Direct Characterization of a Catalytic Surface Reaction Step: Benzene-Deuterium Exchange on Pt(110),'' *Surface Sci.*, **126**, 349 (1983).

Surman, M., S. R. Bare, P. Hofmann, and D. A. King, ''The Influence of Orientation on the H-D Exchange Reactions in Chemisorbed Aromatics: Benzene and Pyridine Adsorbed on Pt(110),'' *Surface Sci.*, **179**, 243 (1987).

Szilagyi, T., ''FTIR Study of Benzene Chemisorption on Pt/SiO_2,'' *J. Mol. Struct.*, **174**, 395 (1988).

Temkin, M. I., D. Y. Murzin, and V. V. Kul'kova, ''Mechanism of the Liquid-Phase Hydrogenation of the Benzene Ring,'' *Kinet. Catal.*, **30**, 637 (1989).

Tetenyi, P., ''Comments on Shawn D. Lin and M. Albert Vannice in Hydrogenation of Aromatic Hydrocarbons over Supported Pt Catalysts,'' *J. Catal.*, **147**, 601 (1994).

Tetenyi, P., and Z. Paal, ''Investigation on the Mechanism of Benzene Hydrogenation: A Radiotracer Study. II. Discussion of the Reaction Mechanism,'' *Z. Phys. Chem. Neue Folge.*, **80**, 63 (1972).

Toppinen, S., T. K. Rantakula, T. Salmi, and J. Aittamaa, ''Kinetics of Liquid-Phase Hydrogenation of Benzene and Some Monosubstituted Alkylbenzenes over a Nickel Catalyst,'' *Ind. Eng. Chem. Res.*, **35**, 1824 (1996).

Toppinen, S., T. K. Rantakyla, T. Salmi, and J. Aittamaa, ''The Liquid-Phase Hydrogenation of Benzene and Substituted Alkylbenzenes over a Nickel Catalyst in a Semi-Batch Reactor,'' *Catal. Today*, **38**, 23 (1997).

Tsai, M. C., C. M. Friend, and E. L. Muetterites, ''Dehydrogenation Processes on Nickel and Platinum Surfaces. Conversion of Cyclohexane, Cyclohexene, and Cyclohexadiene to Benzene,'' *J. Amer. Chem. Soc.*, **104**, 2539 (1982).

van Meerten, R. Z. C., A. C. M. Verhaak, and J. W. E. Coenen, ''Gas-Phase Benzene Hydrogenation on a Nickel-Silica Catalyst: 2. Gravimetric Experiments of Benzene, Cyclohexene, and Cyclohexane Adsorption and Benzene Hydrogenation,'' *J. Catal.*, **44**, 217 (1976).

van Meerten, R. Z. C., and J. W. E. Coenen, ''Gas-Phase Benzene Hydrogenation on a Nickel-Silica Catalyst: 4. Rate Equations and Curve Fitting,'' *J. Catal.*, **46**, 13 (1977).

van Meerten, R. Z. C., T. F. M. de Graaf, and J. W. E. Coenen, ''Gas-Phase Benzene Hydrogenation on a Nickel-Silica Catalyst: 3. Low-Field Magnetization Measurements on Hydrogen, Benzene, Cyclohexene, and Cyclohexane Adsorption, and Benzene Hydrogenation,'' *J. Catal.*, **46**, 1 (1977).

van Meerten, R. Z. C., A. Morales, J. Barbier, and R. Maurel, ''Isotope Effects in the Hydrogenation and Exchange of Benzene on Platinum and Nickel,'' *J. Catal.*, **58**, 43 (1979).

van Meerten, R. Z. C., and J. W. E. Coenen, ''Gas-Phase Benzene Hydrogenation on a Nickel-Silica Catalyst: 1. Experimental Data and Phenomenological Description,'' *J. Catal.*, **37**, 37 (1995).

Vannice, M. A., S. H. Hyun, B. Kalpakci, and W. C. Liauh, ''Entropies of Adsorption in Heterogeneous Catalytic Reactions,'' *J. Catal.*, **56**, 358 (1979).

Wong, K. F., and C. A. Eckert, ''Solvent Design for Chemical Reactions,'' *Ind. Eng. Chem. Process Des. Develop.*, **8**, 568 (1969).

Yu, Y. F., J. J. Chessick, and A. C. Zettlemoyer, ''Adsorption Studies on Metals. VIII. Monofunctional Organic Molecules on Reduced and Oxide-Coated Nickel and Copper,'' *J. Phys. Chem.*, **63**, 1626 (1959).

Manuscript received Oct. 19, 1998, and revision received Feb. 18, 1999.